

First-principles studies of small arsenic interstitial complexes in crystalline silicon

Yonghyun Kim,^{1,*} Taras A. Kirichenko,² Ning Kong,¹ Graeme Henkelman,³ and Sanjay K. Banerjee¹

¹*Microelectronics Research Center, Department of Electrical and Computer Engineering, The University of Texas at Austin, Austin, Texas 78758, USA*

²*Freescale Semiconductor Inc., 3501 Ed Bluestein Blvd., Austin, Texas 78721, USA*

³*Department of Chemistry and Biochemistry, The University of Texas at Austin, Austin, Texas 78712, USA*

(Received 24 March 2008; revised manuscript received 2 December 2008; published 2 February 2009)

We present a first-principles study of the structure and dynamics of small As-interstitial complexes (AsI_2 , As_2I_2 , AsI_3 , and As_2I_3) in crystalline Si. These complexes can be important components of stable As-interstitial clusters or play a key role in interstitial-mediated formation of As-vacancy clusters. Neutral AsI_2 and As_2I_2 are identified as fast-diffusing species that contribute to As transient enhanced diffusion. We demonstrate that the extended defect configuration $\text{As}_2\text{I}_3^{\text{ext}}$ is a stable configuration with a binding energy of 2.64 eV. $\text{As}_2\text{I}_3^{\text{ext}}$ can serve as a nucleation site and facilitate the formation of larger As-interstitial clusters in presence of excess Si interstitials and high As concentration. We also discuss the implications of our findings on As transient enhanced diffusion and clustering and highlight the role of small As-interstitial complexes in ultrashallow junction formation.

DOI: [10.1103/PhysRevB.79.075201](https://doi.org/10.1103/PhysRevB.79.075201)

PACS number(s): 61.72.uf, 85.30.Tv, 71.15.Mb, 71.15.Pd

I. INTRODUCTION

Aggressive complementary metal oxide semiconductor field effect transistors (MOSFETs) scaling requires both ultrashallow junctions and low sheet resistance to overcome short channel effects and enhance the device performance in MOSFETs.¹ It is predicted by the International Technology Roadmap for Semiconductors (ITRS) that ultrashallow junctions less than 5 nm in depth will be necessary to produce the next generation of silicon transistors.¹ In order to achieve these challenging goals, the *n*-type dopant As is a desirable candidate due to its high mass, high solubility, low diffusivity and high activation. However, As also exhibits electrical deactivation and transient enhanced diffusion (TED) during postimplantation thermal annealing.²⁻⁷

Earlier experimental and theoretical studies have shown that As TED can be mainly explained by vacancy-mediated As diffusion⁵⁻⁷ and As deactivation might be driven by As_nV_m complexes.⁸⁻¹¹ However, Kong *et al.*^{4,12} and others have reported that interstitial-mediated As diffusion is dominant for As TED under supersaturated interstitial conditions. In the presence of excess Si interstitials, it is predicted that As_nV_m complexes are easily annihilated by I-V recombination.¹³ Hence, from the recent experimental results, it is clear that I-mediated As diffusion can be very important, together with V-mediated As diffusion.²⁻⁴ In addition, previous experimental results have shown that As doping affects the size and density of Si {311} extended defects by trapping Si interstitials, suggesting that stable As_nI_m complexes are present at intermediate steps of anneal.¹⁴

In presence of excess Si interstitials introduced during ion implantation, I_2 and I_3 clusters can exist in large numbers and be highly mobile under nonequilibrium conditions,¹⁵⁻¹⁷ implying a significant contribution to As TED and I_n cluster formation.²⁻⁷ Likewise, one can expect that small As_nI_m complexes have an important role in As TED and larger As_nI_m cluster formation, especially under Si interstitial supersaturation and high As concentrations. Harrison *et al.*¹⁸ have

reported a possible formation and binding-energy map of small As_nI_m complexes. However, little is known about the detailed structure, stability, and dynamics of the complexes.

In this paper, we present first-principles studies for the structure and dynamics of small As_nI_m complexes (AsI_2 , As_2I_2 , AsI_3 , and As_2I_3) in crystalline Si. Using density-functional theory calculations, we determine the ground-state structures and the minimum-energy diffusion pathways/barriers of small As_nI_m complexes, elucidating their relative roles in As TED and clustering.

II. COMPUTATIONAL DETAILS

All of our atomic and electronic structure calculations based on density-functional theory (DFT) were done using plane-wave basis ultrasoft pseudopotential (USPP) method with the Vienna *Ab-initio* simulation package (VASP).¹⁹⁻²¹ The exchange-correlation energy functional is represented using the generalized gradient approximation (GGA) form of Perdew and Wang (PW91).²² Total-energy calculations were performed on a $2 \times 2 \times 2$ Monkhorst-Pack grid of *k* points in the simple-cubic cell.²³ The optimized Si lattice constant for our system is 5.457 Å. We used a cutoff energy of 200 eV for the plane-wave basis set. A 216-atom supercell was found to sufficiently reduce system size errors in the total energy. All atoms were fully relaxed using the conjugate gradient method to minimize the total energy.

To test convergence with respect to *k*-point sampling and energy cutoff, we perform calculations with a $4 \times 4 \times 4$ *k*-point grid and a 300 eV energy cutoff and find that our calculated formation energies vary by less than 0.2 eV, and our energy barriers by less than 0.03 eV. Local density of states (LDOS) are calculated in order to analyze defect characteristics such as the presence of gap states, their location with respect to the Fermi energy (E_F), and the presence of resonance states in the conduction band. LDOS calculations are done with a $3 \times 3 \times 3$ *k*-point sampling of Brillouin zone. LDOS for different supercells are aligned using deep 2s lev-

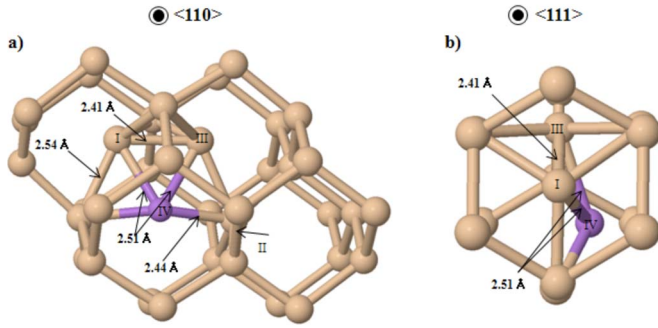


FIG. 1. (Color online) The ground-state structure of AsI_2 viewed from the $\langle 110 \rangle$ and $\langle 111 \rangle$ directions. Yellow (light) and purple (dark) represent Si and As atoms, respectively.

els of bulk Si atoms, distant from the defect structure. We calculate diffusion pathways and barriers using the nudged elastic band method.²⁴ To analyze the electronic structure and characterize bonding properties of stable As_nI_m complexes as well as saddle points for diffusion pathways, we have performed a Bader analysis²⁵ where the atomic volumes are defined solely from the electronic charge density. For this analysis, core charges are included within the projector augmented wave (PAW) framework, and the resolution of the charge-density grid is increased to give Bader charges with high accuracy. We calculated an electron localization function (ELF) isosurface at the value of 0.80.²⁶ In order to calculate the formation energy in different charged states, we applied a monopole charge correction of 0.11 eV in our 216 atom supercell to compensate for the artificial uniform background countercharge required to maintain charge neutrality.²⁷ We used the experimental Si band gap of 1.2 eV to evaluate the chemical potential of electrons since DFT underestimates the gap.²⁷

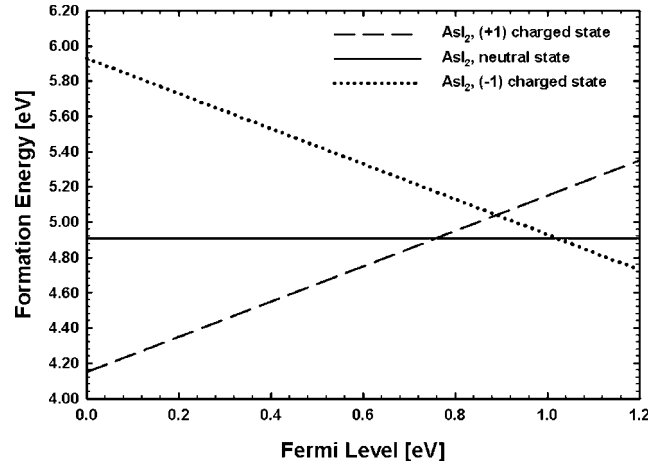


FIG. 2. Formation energy as a function of Fermi level for the minimum-energy configuration of AsI_2 .

III. RESULTS AND DISCUSSION

A. Di-interstitials with one arsenic atom (AsI_2)

We first investigated the lowest energy structure of the neutral di-interstitial with one As atom (AsI_2) and its diffusion pathway in crystalline Si. Several theoretical studies have shown that Si di-interstitials (I_2) are fast-diffusing species with a low migration barrier.^{15,17} In analogy to the Si di-interstitial, AsI_2 is also expected to be highly mobile. The lowest energy configuration identified is shown in Fig. 1.¹⁵ While I_2 has equilateral triangular shape as the ground state, the overall triangular shape of AsI_2 is slightly distorted with the addition of an As atom to the structure. As a result, the Si-Si (I–III) bond length is 2.41 Å and the As-Si (I–IV) bond length is 2.51 Å in the relaxed structure.

We assessed the stability of neutral AsI_2 in crystalline Si by its relative formation energy.²⁸ The formation energy in

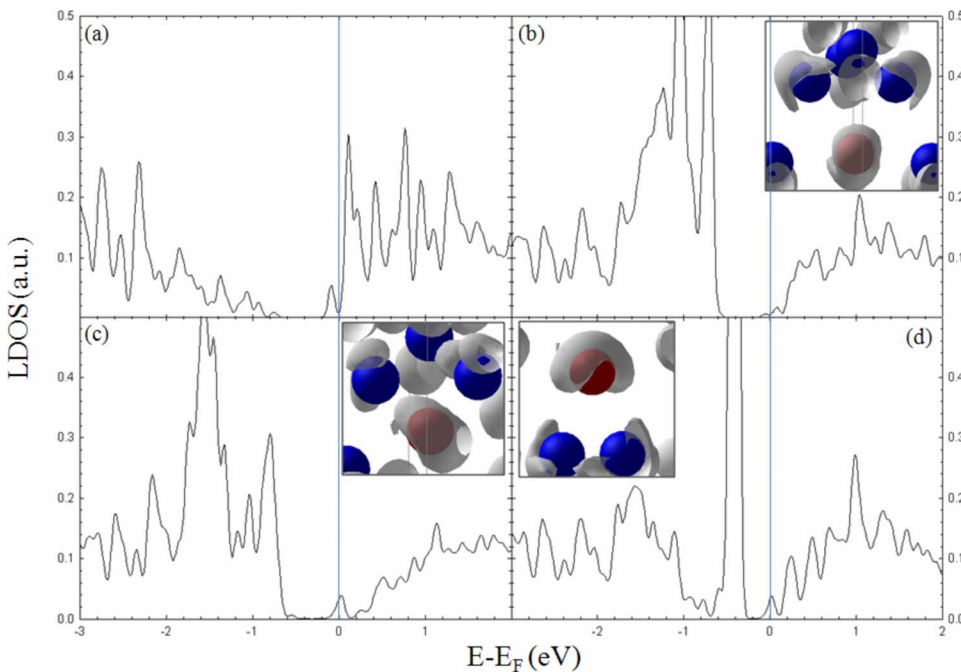


FIG. 3. (Color online) Local density of states (LDOS) of (a) substitutional As (red color) in crystalline Si. LDOS for interstitial As (red color) in (b) global minimum of AsI_2 in Fig. 1. LDOS for interstitial As (red color) in transition states of AsI_2 : (c) T_{AB} and (d) T_{BC} shown in Fig. 4. The zero in horizontal axis ($E - E_F$) corresponds to the calculated Fermi level associated with the structure. The corresponding decomposed electron densities are displayed in the inset with the ELF isosurface with a value of 0.80. Blue and red represent Si and As atoms, respectively.

the neutral state is 4.91 eV for the relaxed configuration shown in Fig. 1. In Fig. 2, the formation energy is calculated as a function of Fermi level, which shows that neutral and negatively charged AsI_2 are stable in lightly and heavily n -doped regions in Si, respectively. The binding energy of AsI_2 is estimated to be 0.56 eV with reference to the dissociation products of neutral I_2 and substitutional As by $E_b(\text{AsI}_2) = E_f(\text{I}_2) + E_f(\text{As}) - E_f(\text{AsI}_2)$. We also calculate the binding energy with reference to the dissociation products of neutral AsI and split- $\langle 110 \rangle$ interstitial (I) and find it to be 1.88 eV by $E_b(\text{AsI}_2) = E_f(\text{AsI}) + E_f(\text{I}) - E_f(\text{AsI}_2)$. Although the “ I_2 and As dissociation” route is more favorable than the “AsI and I dissociation” route, the most probable result of AsI_2 dissociation is expected to be I and AsI in the Si lattice because both I and AsI are highly mobile. It should be noted that it is challenging to show a complete dissociation dynamics for given arsenic-interstitial clusters. For example, the dissociation for AsI_2 pair can be the combinatorial constituents of I and AsI. In the arguments for AsI_2 dissociation, we would like to show two possible dissociated pairs while the binding energies for two cases are shown. Although I_2 (+As) itself is known for fast diffusers, I+AsI seems to be more promising due to their higher concentrations and configurational entropy effect. Moreover, readers can pick up the binding energy with their own discretion based on our discussions.

In order to characterize the bonding of stable AsI_2 , we calculated the LDOS for the As atom in the cluster structure and compared it with that of substitutional As. Figures 3(a) and 3(b) show the band-gap portion of the LDOS for an As atom in a substitutional position and in the cluster, respectively. The LDOS in Fig. 3(b) has a high intensity peak close to the valence-band edge, corresponding to a lone electron pair from the ELF. A Bader analysis, summarized in Table I, shows 5.6 valence electrons for stable AsI_2 in the neutral state when a substitutional As has 5.7 valence electrons. No significant charge transfer to As is found in the positively and negatively charged states of AsI_2 as compared to the neutral state.

Next we propose a diffusion pathway for AsI_2 that occurs through three local minima, labeled as A, B, and C, in Fig. 4. Du *et al.*¹⁵ suggested a novel diffusion pathway of I_2 with a migration barrier of 0.30 eV, with a mechanism consisting of a translation and/or rotation and then a reorientation step. The diffusion pathway of AsI_2 might follow a similar trajectory to I_2 because the structures of AsI_2 and I_2 are very similar. In Fig. 4, the ground-state configuration A is rotated roughly by 60 degrees with respect to the axis connecting both Si (I) and Si (II) atoms in order to reach another local minimum B. At the transition state T_{AB} , the rotational and translational movements of both Si(III) and As(IV) atoms are made from one Si lattice site to another. The reorientation mechanism of the As atom is shown from B to C through the transition state T_{BC} . The As(IV) atom is rotated roughly by 60 degrees about an axis connecting the Si(I) and Si(II) atoms, without affecting the atomic position of Si(III).

The LDOS of the As atom in the saddle-point structures reveals some interesting features of the diffusion pathway. Figure 3(c) is from the saddle point of $\text{AsI}_2(T_{AB})$ in Fig. 4) and Fig. 3(d) is from the saddle point of $\text{AsI}_2(T_{BC})$ in Fig. 4).

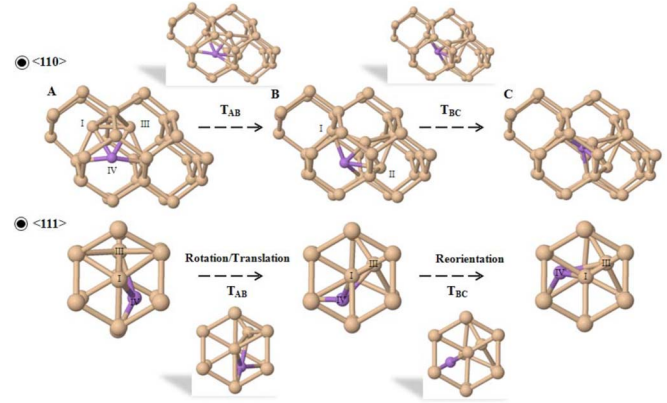


FIG. 4. (Color online) AsI_2 diffusion pathway in crystalline Si. The As atom is labeled as IV, while its neighboring Si atoms are labeled as I, II, and II. Yellow (light) and purple (dark) represent Si and As atoms, respectively.

The As atom in Fig. 3(c) has 6.2 valence electrons at the saddle point. However, this increased charge state (see Table I) does not lead to a substantial increase in the total energy. Upon migration from A to B (see Fig. 4), charge is locally relocated between the As and Si atoms in the T_{AB} structure leading to formation of electron lone pair on As atom and increase in total energy. As shown in Fig. 3(d), the high peak in the band-gap contributes to increasing the total energy at the transition state T_{BC} . Charge transfer at the transition state suggests that AsI_2 migration may start in neutral state, capture an electron, becoming AsI_2^{2-} between A and T_{AB} points, and lose the electron between T_{AB} and B. The viability of such recharging diffusion mechanism will depend on the position of Fermi level. The migration barrier of AsI_2 is shown in Fig. 5 for the translation and/or rotation and reorientation mechanism. The rotation and/or translation barriers from A to B are calculated to be 0.21 eV, and the reorientation barrier from B into C is 0.36 eV. Since AsI_2 has a low migration barrier, it is expected to be highly mobile and diffuse isotropically, similar to I_2 .

TABLE I. Number of valence electrons obtained from Bader decomposed charge analysis on As-interstitial atom of AsI_2 and As_2I_2 in the neutral state. If (-1) and (+1) are specified, they are representing negatively and positively charged state, respectively.

Number of valence electrons		
As substitutional		
As	5.7	
As interstitial		
AsI_2 -“A”	5.6[5.6(-1), 5.6(+1)]	
AsI_2 -“ T_{AB} ”	6.2	
AsI_2 -“ T_{BC} ”	5.6	
	As(I)	As(II)
As_2I_2 -“A”	5.8[5.8(-1), 5.7(+1)]	5.9[5.9(-1), 5.8(+1)]
As_2I_2 -“B”	5.4	5.4
As_2I_2 -“C”	5.4	5.4

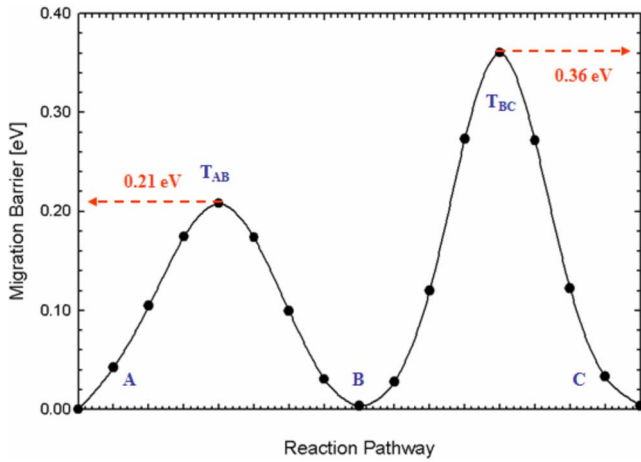


FIG. 5. (Color online) Migration barrier along the As_2I_2 diffusion pathway, calculated with the nudged elastic band method.

B. Di-interstitials with two arsenic atoms (As_2I_2)

We next investigated the structure of the neutral di-arsenic interstitial (As_2I_2) in crystalline Si. Starting with several stable configurations of I_2 ,^{15,29} an extensive search of energetically favorable configurations of As_2I_2 was done in order to identify the global minima. We assessed the stability of neutral As_2I_2 in Si by the relative formation energy.³⁰ Based on the structural configurations in Fig. 6, the formation energies for (a), (b), and (c) are given by 3.90, 4.07, and 4.15 eV in the neutral state, respectively. Our identified atomic structure of As_2I_2 in Fig. 6(a) is more energetically favorable by 0.52 eV in terms of formation energy, as compared to previous calculations.¹⁸ In Fig. 7, the formation energy is calculated as a function of Fermi level, which shows that neutral As_2I_2 is stable in both lightly and heavily n -doped Si.

Consideration of the two local minima [(b) and (c) in Fig. 6] helps us identify the relative roles of chemical bonding and symmetry for the stabilization of As_2I_2 structures. Starting with the global minimum configuration [Fig. 6(a)], we can clearly observe that the most stable structure is highly symmetric and well bonded. A possible reason for the stabilization is that both the Si and As atoms in the global minimum have formed highly symmetric, sp^3 -like bond configurations. The sp^3 -like hybridization is supported by the fact that the sum of bond angles between the As atom and its three neighboring Si atoms is 324.3; close to the sum of angles ($3 \times 109 = 327$). As is evident from the absence of sharp peaks near or in the band gap in Fig. 8(b), this pair is fully involved in bonding with neighboring atoms.

Next, we consider the local minimum As_2I_2 configurations of (b) and (c) in Fig. 6. The bonding of the Si atoms in Fig. 6(b) preserves sp^3 -like hybridization, while that of the As atoms starts to deviate from it, resulting in a sharp peak in the LDOS close to the valence band, with corresponding antibonding resonance level in the conduction band, and a total energy increase of 0.17 eV. In the local minimum structure [Fig. 6(c)], which is next highest in energy to structure Fig. 6(b), the symmetric bonding is lost for both Si and As atoms, increasing the occupation of nonbonded states, and the total energy to 0.25 eV above the global minimum struc-

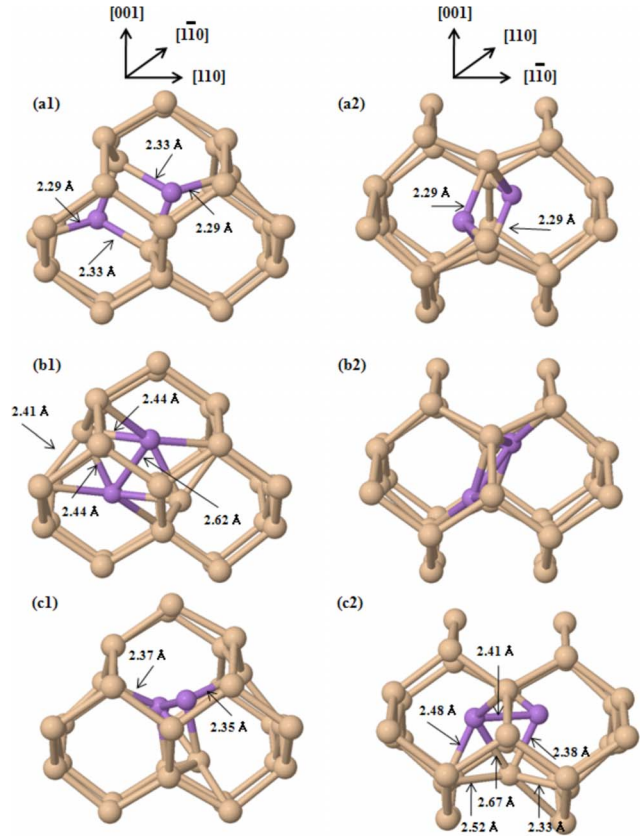


FIG. 6. (Color online) Atomic configurations of As_2I_2 in the $\langle 110 \rangle$ and $\langle 111 \rangle$ directions: (a1) the lowest energy configuration, (b1) and (c1) local minimum configuration. As is shown with purple (dark) atom and Si is shown with yellow (light) atom.

ture [Fig. 6(a)]. From the Bader analysis in Table I, the As atoms in the two configurations in Fig. 6(b) and Fig. 6(c) are locally donating their valence electrons into the neighboring Si atoms.

For the sake of completeness, we estimate the binding energy of the neutral As_2I_2 . The ground state Fig. 6(a) binding is estimated to be 1.90 eV with respect to the dissociation

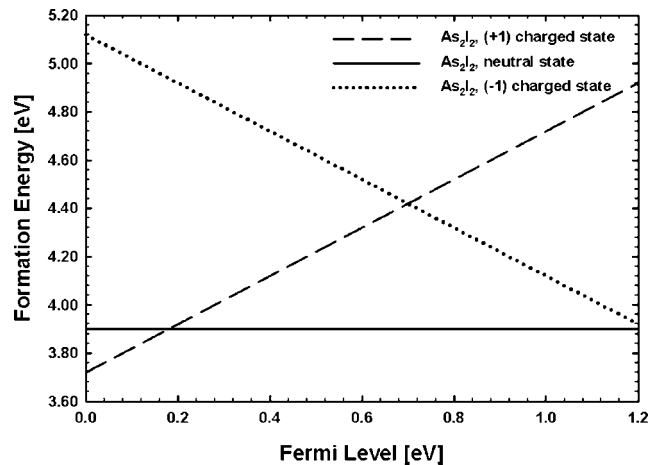


FIG. 7. Formation energy as a function of Fermi level for minimum-energy configuration of As_2I_2 . The experimental band gap for Si is used by 1.2 eV.

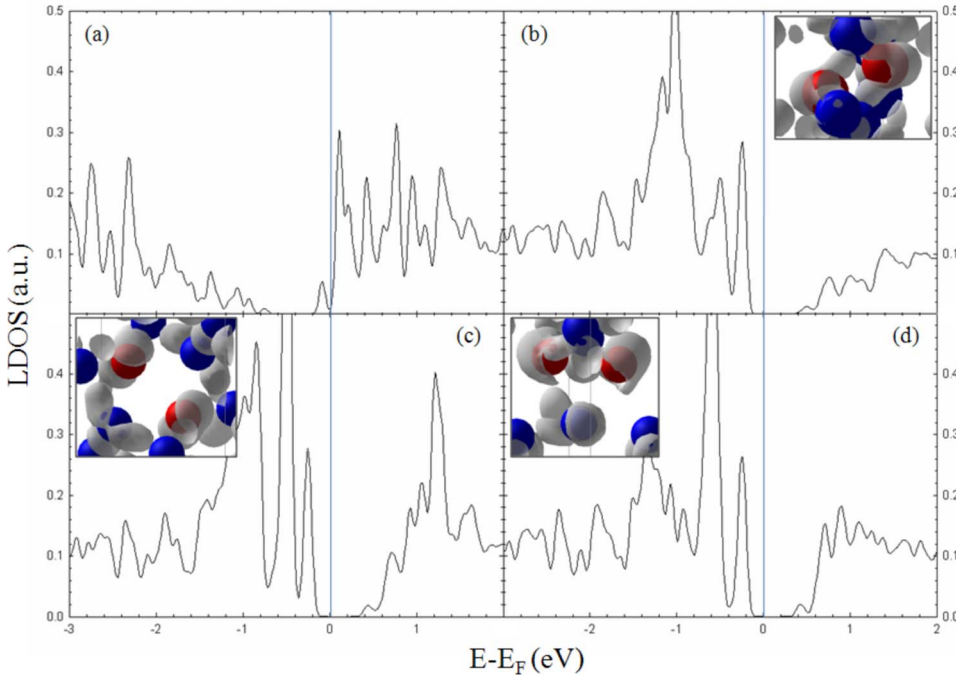


FIG. 8. (Color online) Local density of states (LDOS) of (a) substitutional As in crystalline Si. LDOS (As_2I_2) of (b) Fig. 6(a), (c) Fig. 6(b), and (d) Fig. 6(c). The zero in horizontal axis ($E-E_F$) corresponds to the calculated Fermi level associated with the structure. The corresponding decomposed electron densities are displayed in the inset with the ELF isosurface with a value of 0.80. Blue (dark) and red (light) represent Si and As atoms, respectively.

products of neutral As_2I and I by $E_b(\text{As}_2\text{I}_2) = E_f(\text{As}_2\text{I}) + E_f(\text{I}) - E_f(\text{As}_2\text{I}_2)$. We also calculate the binding energy of As_2I_2 with reference to two neutral AsI and find it to be 2.19 eV by $E_b(\text{As}_2\text{I}_2) = E_f(\text{AsI}) + E_f(\text{AsI}) - E_f(\text{As}_2\text{I}_2)$. With the assumption that the dissociation rate of As_2I_2 is highly dependent on both the mobility of the leaving species and the binding energy, dissociation products of two neutral AsI are expected since AsI is highly mobile. In addition, there are four degenerate states [Fig. 6(c)], which participate in the reorientation mechanism shown in Fig. 9. With an energy barrier of 0.32 eV, As_2I_2 can translate among these four degenerate configurations.

We propose a diffusion pathway for As_2I_2 that occurs through three local minima, labeled as A [Fig. 6(a)], B [Fig. 6(b)], and C [Fig. 6(c)], in Fig. 10. The lowest energy structure of As_2I_2 is given by A (and the equivalent A^\dagger). In order to reach the first transition state T_{AB} from the ground-state configuration A, As(I) and As(II), which are closely aligned along [110], are slightly rotated around the axis connecting the two As atoms. Rotation and translation of the two As atoms results in a reduction in the distance between them, from 3.18 to 2.62 Å. The final state of this process is the next local minimum B in Fig. 10.

To reach the second transition state T_{BC} from the local minimum B, one of two Si atoms that are bonded together with two As atoms, is shifted into the $\langle 111 \rangle$ direction, allowing them to share the lattice site. During the transition of T_{BC} , As(I) and As(II) are rotated into the $[1\bar{1}0]$ direction to form a triangular shape with a Si atom in the direction of the displacement. With a transformation into B, two As atoms are rotated by almost 90 degrees with respect to original ground-state position A, aligning them in the $[1\bar{1}0]$ direction. In the local minimum B, the bond distance of As(I) and As(II) is 2.41 Å, which is smaller than for any other configuration.

In local minimum C, there are four degenerate states as depicted in Fig. 9. In order to reach one of these degenerate

states, C^\dagger , the Si atom just below two As atoms is required to be shifted into the opposite [110] direction with a slight translational movement of these atoms. Next, As(I) and As(II) diffuse through $T^{B^\dagger C^\dagger}$ (equivalent to T^{BC}) to reach the local minimum B^\dagger (equivalent to B). Then they migrate through $T^{A^\dagger B^\dagger}$ (equivalent to T^{AB}) to get to the global minimum A^\dagger .

The diffusion mechanism of As_2I_2 is identified with translation and rotation in their structures with a migration barrier, as shown in Fig. 11. The initial barrier from A to B configurations is calculated as 1.03 eV. The barrier from B to C is 0.42 eV. Then, reorientation occurs with a migration barrier

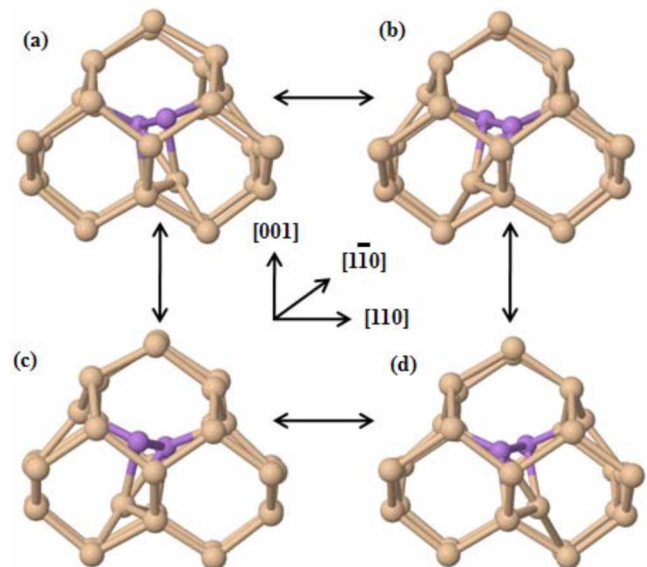


FIG. 9. (Color online) Reorientation mechanism of As_2I_2 within a lattice site. All four configurations are degenerate in total energy. As is depicted with purple (dark) atom and Si is shown with yellow (light) atom.

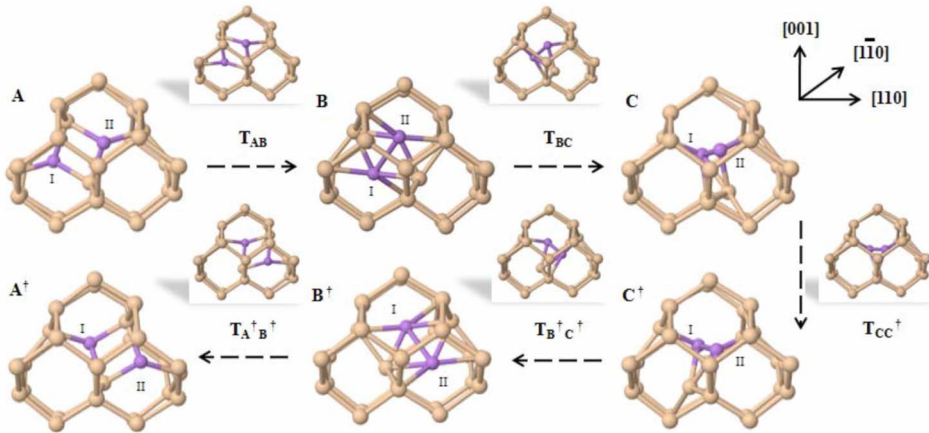


FIG. 10. (Color online) As_2I_2 diffusion pathway in crystalline Si. A is the ground state while B and C are the local minimum states. Transition states are also shown. The two As atoms are labeled as I and II.

of 0.32 eV. Although the local minimum B has a slightly higher relative energy by 0.16 eV than the ground state A, the partial diffusion pathway can be composed of B (B^\dagger) and C (C^\dagger) with low energy barrier of 0.42 eV.

C. Tri-interstitials with one and two arsenic atoms

We obtained structural configurations and formation energies for AsI_3 and As_2I_3 clusters. Figure 12 shows that the lowest energy configuration for neutral compact type tri-interstitials with one As atom (AsI_3^c) in crystalline Si.^{16,31} The ground state AsI_3^c in Fig. 12(a) has a bond length of 2.37 and 2.43 Å for the Si-Si(III-IV) and As-Si(III-V) bonds, respectively. The transition state of AsI_3^c , shown in Fig. 12(b), has a similar configuration to I_3^c ; with comparable As-Si and Si-Si bond lengths of 2.56 and 2.51 Å, respectively. We assessed the formation energy of AsI_3^c to be 6.71 eV in Fig. 12(a). The stable AsI_3^c structure is formed by displacing the two silicon atoms in the I_3^c cluster away from the base of equilateral triangle in $\langle 111 \rangle$ direction. The binding energy of AsI_3^c is estimated to be 1.96 eV with respect to the dissociation products of neutral I and AsI_2 by $E_b(AsI_3^c) = E_f(I) + E_f(AsI_2) - E_f(AsI_3^c)$.

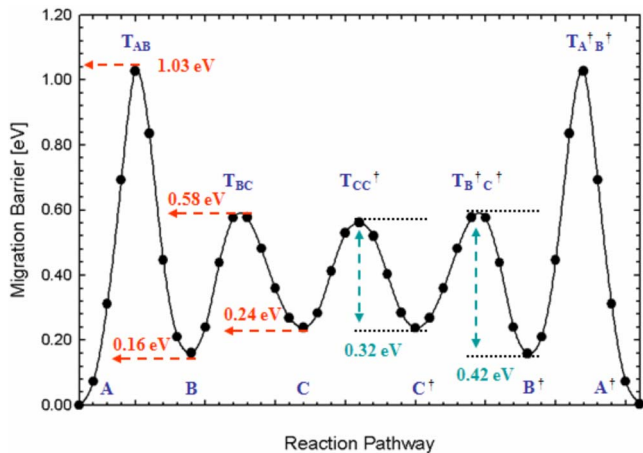


FIG. 11. (Color online) Migration barrier along the As_2I_2 diffusion pathway in crystalline Si.

When an As atom replaces one of the Si interstitial atoms in I_3^c it does not distort the bond configurations significantly, as shown in Fig. 12, and AsI_3^c exhibits a similar reorientation behavior as I_3^c , as shown in Fig. 13. We find that the rotation barrier for AsI_3^c is 0.39 eV while a reorientation barrier is just 0.10 eV (see Fig. 14). The 60 degree rotation of AsI_3^c occurs by a screw motion between two local minima which are labeled A and B in Fig. 13. The ground state A and B can move into a nearest-neighbor lattice site by the transition state “ R_A ” and “ R_B ,” respectively. However, As(V) has limited space to reorient its position while maintaining the overall atomic configuration of AsI_3^c , which, unlike I_3^c , implies anisotropic diffusion. Hence our calculations show that the dynamics of compact AsI_3^c will be dominated by dissociation as well as reorientation of the cluster. Next, we consider an extended AsI_3^{ext} configuration. The lowest energy configuration of AsI_3^{ext} is found to have a formation energy of 6.00 eV, as shown in Fig. 15(a). The binding energy is calculated to be 2.67 eV with respect to the dissociation products of neutral I and AsI_2 by $E_b(AsI_3^{ext}) = E_f(I) + E_f(AsI_2) - E_f(AsI_3^{ext})$.

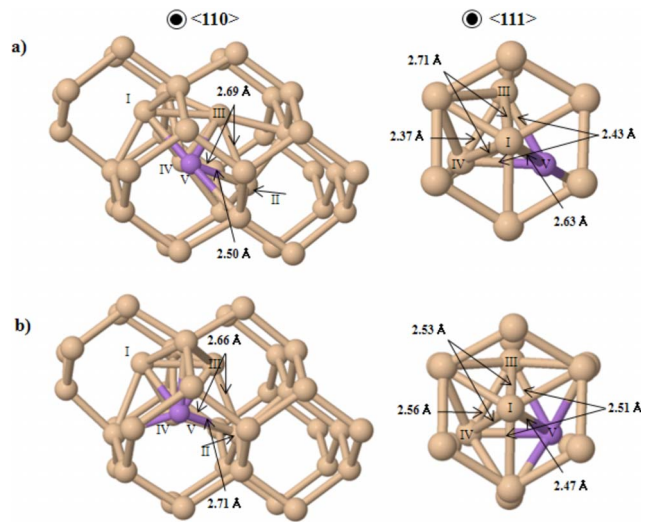


FIG. 12. (Color online) Atomic configurations and bond lengths of AsI_3^c in $\langle 110 \rangle$ and $\langle 111 \rangle$ directions: (a) the lowest energy configuration, (b) the transition-state configuration. As is depicted with purple (dark) atom and Si is shown with yellow (light) atom.

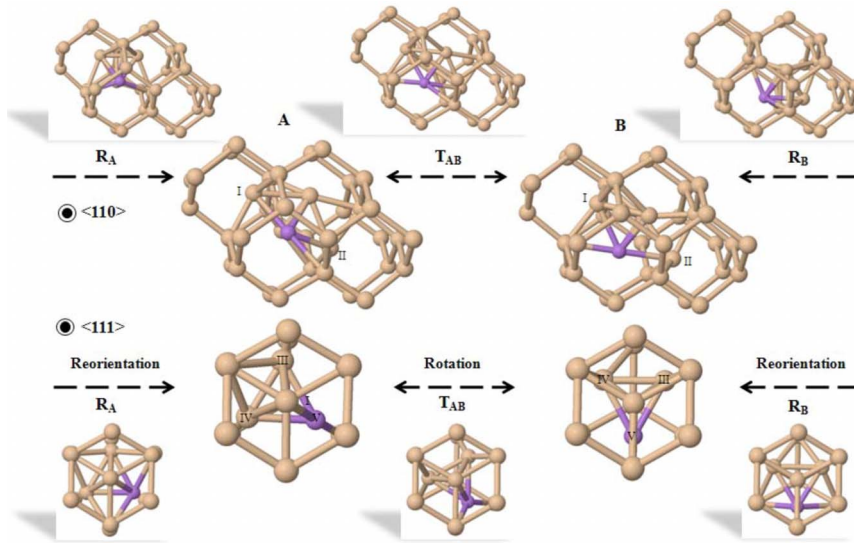


FIG. 13. (Color online) AsI_3^c diffusion pathway in crystalline Si. The local minimum structures (A and B) are shown with intermediate transition states.

Finally, we investigate the relative stability of interstitials with two As atoms within both compact ($As_2I_3^c$) and extended structures ($As_2I_3^{ext}$). The lowest-energy configuration of $As_2I_3^c$ is shown in Fig. 16 with a formation energy of 5.95 eV. The binding energy of $As_2I_3^c$ is estimated at 2.05 eV with respect to the dissociation products of neutral AsI and AsI_2 . The propensity of $As_2I_3^c$ to easily dissociate is explained by the relatively large distance of 2.98 Å between As(V) and As(VI).

The lowest-energy configuration of $As_2I_3^{ext}$ is shown in Fig. 15(b) with a formation energy of 5.36 eV. The binding energy of $As_2I_3^{ext}$ is estimated to be 2.64 eV with respect to the dissociation products of neutral AsI and AsI_2 . The bond length between the As atom and the three neighboring Si atoms is 2.31 Å, which shows highly symmetric bonding characteristics. The As atoms and their neighboring Si atoms have a stable bonding geometry in $As_2I_3^{ext}$, which is similar to the extended type I_3^{ext} .

D. Implications on interstitial-mediated arsenic diffusion and clustering

Harrison *et al.*¹³ suggested the easy annihilation of arsenic-vacancy complexes due to interstitial-vacancy re-

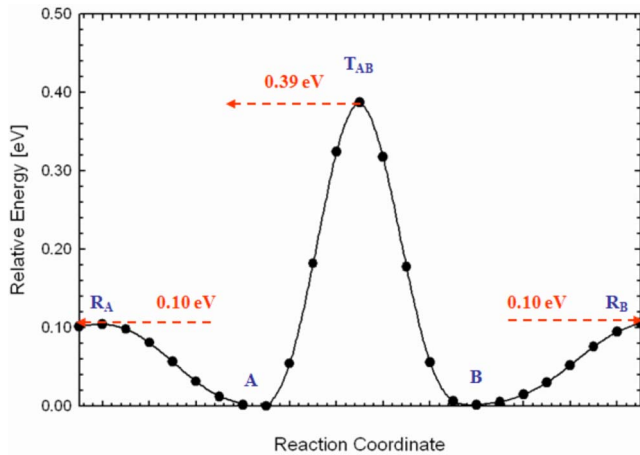


FIG. 14. (Color online) Migration barrier along with AsI_3^c diffusion pathway in crystalline Si.

combination in the presence of excess interstitials. Depending on which defect is in excess, the relative role of interstitial- and vacancy-mediated diffusion in As TED can be determined.⁸ Kong *et al.*¹² suggested that interstitial-mediated As diffusion could be dominant with excess Si interstitials, controlling initial interstitial and vacancy concentrations. Moreover, Brindos *et al.*¹⁴ showed that the number and size of {311} extended defects is reduced as As doping concentration is increased, suggesting the existence of stable arsenic-interstitial complexes at 750 °C.

In order to investigate the implications of arsenic-interstitial complexes for As TED and clustering, *ab-initio* density-functional theory calculation results for formation, binding, and migration energy of arsenic-interstitial complexes are summarized in Table II. Here, we have calculated the formation energy of each cluster with respect to three reference states; E_{f1} has a reference state of substitutional As atoms and a perfect Si lattice,³² E_{f2} has a reference state of substitutional As and n interstitial Si atoms in the Si lattice,³³ and E_{f3} has a reference state of substitutional As and n interstitial Si atoms in the {311} extended defects whose formation energy per atom is approximately 2 eV.^{34,35} E_{f1} describes the energetic cost to form clusters from a perfect crystal—these energies are very high because of the high cost of forming interstitials. E_{f2} does not include the cost of forming the interstitials, which is appropriate in the limit where there is a high concentration of interstitials in the lattice. In this

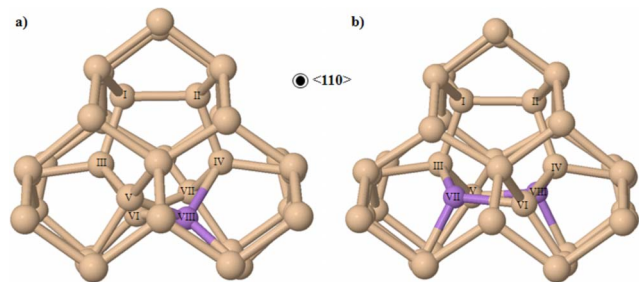


FIG. 15. (Color online) Lowest energy structure of (a) AsI_3^{ext} and (b) $As_2I_3^{ext}$. As is depicted as purple (dark) atom and Si is shown as yellow (light) atom.

limit, As_nI_m clusters are increasingly stable with cluster size. Since experimental conditions will lie somewhere between these two limits (E_{f1} and E_{f2}), E_{f3} considers the energetic cost of available interstitials from $\{311\}$ extended defects which are formed by excess Si interstitials under nonequilibrium conditions during thermal annealing.

Even though As_nI_m clusters are energetically stable in the presence of excess interstitials, there is an entropic cost to forming these clusters. At high temperatures and low As and/or interstitial concentrations, entropy will favor smaller clusters. This configurational entropy can be estimated from the equilibrium concentration of Si-free interstitials (C_1^*), taken to be $7.95 \times 10^{27} \exp(-4.002/kT) \text{ cm}^{-3}$.³⁶ Because the defect concentrations in Si after ion implantation are not explicitly known and they highly depend on implant process conditions, the equilibrium concentrations are assumed as an extreme case in order to demonstrate a configurational entropy effect in the clusters. Here, we are assuming that the As concentration is higher than that of the Si interstitials under the high As dose ($>5 \times 10^{14} \text{ cm}^{-2}$) conditions used for junction formation. Then, the configurational entropy (S) of bringing each additional interstitial into a cluster will be dominated by $k \ln(C_1^*/C_{\text{Si}})$. At 1000 K, this configurational entropy increases the free energy of formation of the clusters by 1.22 eV per interstitial; the values ($E_{f3}-\text{TS}$) are shown in Table II. Therefore, larger clusters are less favorable due to the configurational entropy.

The compact configurations of AsI_3^c and As_2I_3^c are expected to dissociate instead of diffuse as a cluster. The neutral AsI_2 can be easily formed with excess Si interstitials and high As concentrations, and AsI has a low migration barrier of (<0.2 eV).³⁷ The relative contribution of AsI_2 and AsI to As TED can be found by evaluating $D(\text{AsI}_2)C(\text{AsI}_2)/D(\text{AsI})C(\text{AsI})$, where C is the defect concentration.³⁸ Using $D=D_0 \exp(-E_m/kT)$ with $E_m(\text{AsI})$

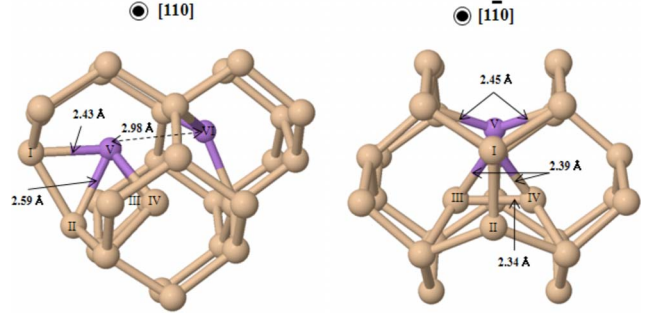


FIG. 16. (Color online) Lowest energy structure of As_2I_3^c . As is depicted as purple atom and Si is shown as yellow atom.

$=0.15$ eV and $E_m(\text{AsI}_2)=0.36$ eV, $D(\text{AsI})$ is approximately one order of magnitude greater than $D(\text{AsI}_2)$ at 1200 K. If $C(\text{AsI}_2)$ is greater in magnitude than $C(\text{AsI})$ at 1200 K with excess Si interstitials under nonequilibrium conditions after ion implantation, AsI_2 (and AsI) could be expected to make a large contribution to As TED. For As_nI_m clustering, the most likely key intermediate states are As_2I_2 and As_2I_3 . Since the migration barrier of AsI is extremely low (<0.2 eV),³⁷ neutral As_2I_2 can be easily formed under excess Si interstitials and high As concentrations. While neutral As_2I_2 is highly mobile and has relatively strong binding energy, it can also evolve into the larger As_2I_3 by reacting with an additional Si interstitial.

Neutral $\text{As}_2\text{I}_3^{\text{ext}}$ has a formation energy of 5.36 eV (E_{f1}) and a strong binding energy of 2.64 eV when there are three additional atoms (Table II). This result implies that the neutral $\text{As}_2\text{I}_3^{\text{ext}}$ is a very stable configuration and a likely key nucleation state for larger arsenic-interstitial clusters. The high migration barrier of $\text{As}_2\text{I}_3^{\text{ext}}$ is required to support it. Unfortunately the diffusion pathway and barrier of $\text{As}_2\text{I}_3^{\text{ext}}$ is hard to determine explicitly due to its complex structure. To

TABLE II. Formation energy (E_{f1} , E_{f2} , and E_{f3}), formation free energy ($E_{f3}-\text{TS}$) at 1000 K, binding energy (E_b), and migration energy (E_m) of neutral mono-, di-, and tri-interstitials with arsenic-interstitial complexes. E_{f1} describes the energetic cost to form clusters from a perfect crystal while E_{f2} does not include the cost of forming the interstitials. E_{f3} considers the energetic cost of available interstitials from $\{311\}$ extended defects which are formed by excess Si interstitials under nonequilibrium conditions during thermal annealing. Energy unit is [eV]. All of them are calculated in $[216+n]$ atom supercell (Refs. 15–18, 29, 31, 37, and 38).

$[216+n]$ atoms	Clusters	E_{f1}	E_{f2}	E_{f3}	$E_{f3}-\text{TS}$	E_b	E_m
$n=1$	I	3.74					0.29
	AsI	3.07	-0.67	1.33	1.33	0.67	0.15
	As_2I	2.00	-1.63	2.37	2.37	1.07	1.33
$n=2$	I_2	5.49	-1.97	2.03	3.25	1.99	0.30
	As I_2	4.91	-2.50	1.50	2.72	1.88	0.36
	As_2I_2	3.90	3.51	0.49	1.71	2.19	1.03/0.42
$n=3$	I_3^c	6.93	-4.25	1.75	4.18	2.30	0.49
	I_3^{ext}	6.28	-4.91	1.09	3.53	2.95	
	AsI_3^c	6.71	-4.50	1.50	3.93	1.96	0.39
	$\text{AsI}_3^{\text{ext}}$	6.00	-5.21	0.79	3.22	2.67	
	As_2I_3^c	5.95	-5.27	0.73	3.17	2.05	
	$\text{As}_2\text{I}_3^{\text{ext}}$	5.36	-5.85	0.15	2.58	2.64	

exclude the possibility of a low diffusion barrier for neutral $\text{As}_2\text{I}_3^{\text{ext}}$ we performed *ab-initio* molecular dynamics (MD) with a 2 fs time step for 50 ps, using a Nose-Hoover thermostat to maintain the temperature at 1000 K. We did not observe a single diffusion event for the entire duration of MD run. In contrast, Estreicher *et al.*¹⁷ have shown by *ab-initio* MD simulation that the diffusion event for I_2 and I_3 can happen within few ps at 1000 K. In addition, an adaptive kinetic Monte Carlo simulation (aKMC) (Ref. 39) was used to extensively search for low energy saddle points, find possible diffusion pathway for $\text{As}_2\text{I}_3^{\text{ext}}$, and calculate the dynamics of this cluster over long time scales. In our aKMC dynamics, $\text{As}_2\text{I}_3^{\text{ext}}$ is seen to exchange rapidly between conformers, crossing a low migration barrier (<1 eV), before breaking up into $\text{AsI}_2 + \text{AsI}$ by crossing a higher barrier (>1 eV). Thus, $\text{As}_2\text{I}_3^{\text{ext}}$ is unlikely to diffuse with low migration barrier less than 1 eV and the energy cost of breaking its bond network configuration should be high.

IV. SUMMARY

We present a first-principles study of the structure and dynamics of small As-interstitial complexes (AsI_2 , As_2I_2 , AsI_3 , and As_2I_3) in Si. The compact type configurations of

AsI_3^{c} and $\text{As}_2\text{I}_3^{\text{c}}$ are expected to dissociate easily and the extended configuration, $\text{As}_2\text{I}_3^{\text{ext}}$, forms a stable bonding network and has a strong binding energy of 2.64 eV. In presence of excess Si interstitials and high As concentration, As_2I_2 could be a key intermediate state, and $\text{As}_2\text{I}_3^{\text{ext}}$ could provide a key nucleation site in the formation of larger As-interstitial clusters. A diffusion mechanism for neutral AsI_2 is proposed with an overall migration barrier of 0.36 eV. Our results show that AsI_2 may significantly contribute to As TED for excess Si interstitials. A diffusion mechanism for neutral As_2I_2 is suggested with an overall migration barrier of 1.03 eV and an intermediate reoriented configuration with an energy of 0.42 eV. This detailed understanding of the relative roles of small As-interstitial complexes can provide valuable guidance for ultrashallow junction engineering.

ACKNOWLEDGMENTS

This work is supported by Semiconductor Research Corporation (SRC). Y. Kim would like to thank Applied Materials Graduate Fellowship for financial support. All our calculations were performed using a supercomputer at the Texas Advanced Computing Center (TACC) at the University of Texas at Austin.

*Author to whom correspondence should be addressed: erogen@gmail.com

¹International Technology Roadmap for Semiconductors, 2007.

²A. Ural, P. Griffin, and J. Plummer, *J. Appl. Phys.* **85**, 6440 (1999).

³R. Kim, T. Hirose, T. Shano, H. Tsuji, and K. Taniguchi, *Jpn. J. Appl. Phys., Part 1* **41**, 227 (2002).

⁴S. Solmi, M. Ferri, M. Bersani, D. Giubertoni, and V. Soncini, *J. Appl. Phys.* **94**, 4950 (2003).

⁵D. Mathiot and J. C. Pfister, *Appl. Phys. Lett.* **42**, 1043 (1983).

⁶M. Ramamoorthy and S. T. Pantelides, *Phys. Rev. Lett.* **76**, 4753 (1996).

⁷J. Xie and S. P. Chen, *Phys. Rev. Lett.* **83**, 1795 (1999).

⁸P. M. Fahey, P. B. Griffin, and J. D. Plummer, *Rev. Mod. Phys.* **61**, 289 (1989).

⁹P. M. Rousseau, P. B. Griffin, and J. D. Plummer, *Appl. Phys. Lett.* **65**, 578 (1994).

¹⁰D. W. Lawther, U. Myler, P. J. Simpson, P. M. Rousseau, P. B. Griffin, and J. D. Plummer, *Appl. Phys. Lett.* **67**, 3575 (1995).

¹¹D. C. Mueller, E. Alonso, and W. Fichtner, *Phys. Rev. B* **68**, 045208 (2003).

¹²N. Kong, S. K. Banerjee, T. Kirichenko, S. Anderson, and M. Foisy, *Appl. Phys. Lett.* **90**, 062107 (2007).

¹³S. A. Harrison, T. F. Edgar, and G. S. Hwang, *Appl. Phys. Lett.* **85**, 4935 (2004).

¹⁴R. Brindos, P. Keys, K. Jones, and M. Law, *Appl. Phys. Lett.* **75**, 229 (1999).

¹⁵Y. A. Du, R. G. Hennig, and J. W. Wilkins, *Phys. Rev. B* **73**, 245203 (2006).

¹⁶Y. A. Du, S. A. Barr, K. R. A. Hazzard, T. J. Lenosky, R. G. Hennig, and J. W. Wilkins, *Phys. Rev. B* **72**, 241306(R) (2005).

¹⁷S. K. Estreicher, M. Gharaibeh, P. A. Fedders, and P. Ordejon, *Phys. Rev. Lett.* **86**, 1247 (2001).

¹⁸S. A. Harrison, T. F. Edgar, and G. S. Hwang, *Electrochem. Solid-State Lett.* **9**, G354 (2006).

¹⁹P. Hohenberg and W. Kohn, *Phys. Rev.* **136**, B864 (1964).

²⁰W. Kohn and L. J. Sham, *Phys. Rev.* **140**, A1133 (1965).

²¹G. Kresse and J. Furthmüller, *VASP the Guide* (Universität Wien, Wien, Austria, 2007); G. Kresse and J. Hafner, *Phys. Rev. B* **47**, 558 (1993).

²²J. P. Perdew and Y. Wang, *Phys. Rev. B* **45**, 13244 (1992).

²³H. Monkhorst and J. Pack, *Phys. Rev. B* **13**, 5188 (1976).

²⁴G. Henkelman, B. Uberuaga, and H. Jónsson, *J. Chem. Phys.* **113**, 9901 (2000).

²⁵G. Henkelman, A. Arnaldsson, and H. Jónsson, *Comput. Mater. Sci.* **36**, 354 (2006).

²⁶A. D. Becke and K. E. Edgecombe, *J. Chem. Phys.* **92**, 5397 (1990).

²⁷J.-W. Jeong and A. Oshiyama, *Phys. Rev. B* **64**, 235204 (2001).

²⁸The formation energy is defined by $E_f = E[\text{Si}_{217}\text{As}] - 217\mu_{\text{Si}} - \mu_{\text{As}}$, where $E[\text{Si}_{217}\text{As}]$ is the total energy of As-interstitial complexes in the 216 atom supercell, μ_{Si} is the energy per atom ($=E[\text{Si}_{216}/216]$) in bulk Si, and μ_{As} is the relative energy per substitutional As atom in defect-free bulk Si ($=E[\text{Si}_{215}\text{As}] - 215\mu_{\text{Si}}$).

²⁹D. A. Richie, J. Kim, S. A. Barr, K. R. A. Hazzard, R. Hennig, and J. W. Wilkins, *Phys. Rev. Lett.* **92**, 045501 (2004).

³⁰The formation energy is defined by $E_f = E[\text{Si}_{216}\text{As}_2] - 216\mu_{\text{Si}} - 2\mu_{\text{As}}$, where $E[\text{Si}_{216}\text{As}_2]$ is the total energy of arsenic-interstitial complexes in the 216 atom supercell.

³¹A. Carvalho, R. Jones, J. Coutinho, and P. R. Briddon, *Phys. Rev. B* **72**, 155208 (2005).

$$^{32}E_{f1}(\text{As}_n\text{I}_m) = E(\text{As}_n\text{I}_m) - (216 + m - n) \times \mu_{\text{Si}} - n \times \mu_{\text{As}}.$$

$$^{33}E_{f2}(\text{As}_n\text{I}_m) = E(\text{As}_n\text{I}_m) - (216 - n) \times \mu_{\text{Si}} - m \times \mu_{\text{I}} - n \times \mu_{\text{As}}, \mu_{\text{I}} \\ = E(\text{Si}_{217}) - 216 \times \mu_{\text{Si}}.$$

$$^{34}E_{f3}(\text{As}_n\text{I}_m) = E_{f2}(\text{As}_n\text{I}_m) + E_f(\{311\}) \text{ per atom.}$$

³⁵J. Kim, J. W. Wilkins, F. S. Khan, and A. Canning, *Phys. Rev. B* **55**, 16186 (1997).

³⁶*Synopsys Sentaurus Advanced Calibration User Guide, Version*

A-2008.09 (Synopsys, Mountain View, CA, 2008), p. 76.

³⁷S. A. Harrison, T. F. Edgar, and G. S. Hwang, *Appl. Phys. Lett.* **87**, 231905 (2005).

³⁸S. A. Harrison, T. F. Edgar, and G. S. Hwang, *Phys. Rev. B* **72**, 195414 (2005).

³⁹L. Xu and G. Henkelman, *J. Chem. Phys.* **129**, 114104 (2008).